IEEE Access
Multidisciplinary | Rapid Review | Open Access Journal

Received July 27, 2021, accepted August 20, 2021, date of publication August 24, 2021, date of current version September 3, 2021.

Digital Object Identifier 10.1109/ACCESS.2021.3107294

Pixel and Object-Based Machine Learning Classification Schemes for Lithological Mapping Enhancement of Semi-Arid Regions Using Sentinel-2A Imagery: A Case Study of the Southern Moroccan Meseta

IMANE SERBOUTI[1], MOHAMMED RAJI[1], MUSTAPHA HAKDAOUI[1], BISWAJEET PRADHAN[2,3], (Senior Member, IEEE), CHANG-WOOK LEE[4], AND ABDULLAH M. ALAMRI[5]

[1]Department of Geology, Laboratory of Applied Geology, Geomatic and Environment, Faculty of Sciences Ben M'Sik, Hassan II University of Casablanca, Casablanca 20000, Morocco
[2]Centre for Advanced Modelling and Geospatial Information Systems (CAMGIS), Faculty of Engineering and Information Technology, University of Technology Sydney, Ultimo 2007, New South Wales, Australia
[3]Earth Observation Centre, Institute of Climate Change, Universiti Kebangsaan Malaysia, Bangi 43600, Malaysia
[4]Division of Science Education, Kangwon National University, Kangwondaehak-gil, Chuncheon-si, Gangwon-do 24341, South Korea
[5]Department of Geology and Geophysics, College of Science, King Saud University, Riyadh 11451, Saudi Arabia

Corresponding authors: Biswajeet Pradhan (biswajeet.pradhan@uts.edu.au) and Chang-Wook Lee (cwlee@kangwon.ac.kr).

This work was supported in part by the Centre for Advanced Modelling and Geospatial Information Systems (CAMGIS), Faculty of Engineering & IT, University of Technology Sydney (UTS), in part by the Basic Science Research Program through the National Research Foundation of Korea (NRF) through the Ministry of Education under Grant 2019R1A2C1085686, and in part by the Researchers Supporting Project, King Saud University, Riyadh, Saudi Arabia, under Grant RSP-2021/14.

ABSTRACT Mapping lithological units of an area using remote sensing data can be broadly grouped into pixel-based (PBIA), sub-pixel based (SPBIA) and object-based (GEOBIA) image analysis approaches. Since it is not only the datasets adequacy but also the correct classification selection that influences the lithological mapping. This research is intended to analyze and evaluate the efficiency of these three approaches for lithological mapping in semi-arid areas, by using Sentinel-2A data and many algorithms for image enhancement and spectral analysis, in particular two specialized Band Ratio (BR) and the Independent component analysis (ICA), for that reason the Paleozoic Massif of Skhour Rehamna, situated in the western Moroccan Meseta was chosen. In this study, the support vector machine (SVM) that is theoretically more efficient machine learning algorithm (MLA) in geological mapping is used in PBIA and GEOBIA approaches. The evaluation and comparison of the performance of these different methods showed that SVM-GEOBIA approach gives the highest overall classification accuracy (OA $\approx$ 93%) and kappa coefficient (K) of 0, 89, while SPBIA classification showed OA of approximately 89% and kappa coefficient of 0, 84, whereas the lithological maps resulted from SVM-PBIA method exhibit salt and pepper noise, with a lower OA of 87% and kappa coefficient of 0, 80 comparing them with the other classification approaches. From the results of this comparative study, we can conclude that the SVM-GEOBIA classification approach is the most suitable technique for lithological mapping in semi-arid regions, where outcrops are often inaccessible, which complicates classic cartographic work.

INDEX TERMS Lithological mapping, sentinel-2A, SVM-GEOBIA, remote sensing, moroccan meseta.

I. INTRODUCTION

The importance of producing geological maps makes the entire branch of remote sensing science one of the well-established information technology in lithological mapping and mineral exploration [1]–[3]. It is a very popular and powerful technique for regional geological classification process, particularly in arid and semi-arid areas [4]. The remotely sensed spectral imagery provides a high potential in overcoming the cost-effective, time-consuming and logistical

The associate editor coordinating the review of this manuscript and approving it for publication was Qiangqiang Yuan.

limitations associated with traditional field-based geological mapping over vast regions [5], [6]. Recent development of multi-spectral remote sensing data such as Sentinel-2A Multi-Spectral Imagery (MSI), launched by the European Space Agency (ESA), has shown a high potential for complex geological and mineral mapping in various parts of the globe [7]–[9].

In combination with multi-spectral satellite imagery for geological mapping, a wide array of classification approaches have been applied, which can be broadly categorized into three main categories; Pixel-Based Image Analysis (PBIA), Subpixel Based Image Analysis (SPBIA) and GEographic Object Based Image Analysis (GEOBIA) [10], [11].

PBIA uses machine learning algorithms (MLAs), by taking into account the approximate fit between the spectral characteristics of the image pixel spectrum and the reference spectra of a known lithological unit, in order to classify each pixel to its litho-class [12], without taking into consideration the spatial context. However, selecting appropriate training samples is considered as an essential stage in PBIA technique to succeed the classification procedure. The MLAs that have been widely used for per-pixel lithological mapping are k-Nearest Neighbor (k-NN), Random forest (RF) and Support Vector Machine (SVM) [13]–[15]. The SVM algorithm was implemented in this research due to its efficiency in geological mapping and great performance in high-dimensional feature space [16], [17]. The main problem encountered by this approach is the intra-class spectral heterogeneity related to land cover such as buildings, vegetation and many surface materials. Consequently, the resultant lithological maps exhibit misclassified pixels that occurs the ''Salt and Pepper'' artifacts, of isolated and spurious pixel classifications, in addition to the poorly defined boundaries [18].

Therefore, in order to overcome the issues related to mixed pixels in the images, Sub-pixel Image Analysis (SPBIA), also termed soft classification, have been widely used in the literature. It consists of deconvolving the image pixel spectra into fractional abundance images of different ground materials [18]. However, the generalized lithological maps generated from various fractional images engenders often difficulties in producing homogeneous maps [19], [20], and also produce an inconsistent generalized thematic results [21]. This technique is seldom applied in lithological mapping but widely used in crop mapping [22], [23].

It was acknowledged in previous studies [24], [25], that a pixel is not the optimal spatial unit for lithological mapping. So due to the limitations encountered by pixel-based and sub-pixel-based approaches [25] as well as the high spatial resolution of Sentinel-2A imagery, the Geographic Object-Based Image Analysis (GEOBIA), also known as Object-Based Image Analysis (OBIA), came into the picture [26]. This approach is basically based on segmenting the image into meaningful and homogeneous objects by combining contiguous and identical like-pixels i.e. the textural and spectral properties [27], [28], thus, image objects accordingly contain supplemental spectral and spatial attributes compared to individual pixels [29]. On the basis of the resultant segmented images, numerous MLAs are applied in GEOBIA approach such as k-NN classifier [30] to extract thematic maps, nevertheless, the supervised classifier support vector machine (SVM) is one of the most effective algorithm in GEOBIA approach for land use land cover mapping (LULC) [31], it has also has been used in this study to evaluate its performance in the field of geological mapping. Consequently, object-based approach has been widely used for several studies, including LULC classification [32], [33], change detection [34], [35], urban mapping [36], landform mapping [37]–[39], and lithological mapping [30], [40]. Furthermore, most publication that used GEOBIA in geological mapping applied either WorldView-3 (WV-3) along with SVM MLA [41], or the Airborne LiDAR (Li), Airborne Thematic Mapper-9 (ATM9) [40] and Sentinel-2A (S2A) datasets using k-NN algorithm in the classification process [30]. Digital image processing tools such as Principal Component Analysis (PCA) [4], [42], Minimum Noise Fraction (MNF) [4], [40], Independent Component Analysis (ICA) [43], [44], Band Ratio (BR) [42], [45] and intensity Hue Saturation (IHS) [46], [47] were extensively used to improve lithological and mineral discrimination, based on enhancing color and features in order to demarcate different rock types.

In this research, we used MLA over the traditional classification approaches based on spectral distance measurement (Mahalanobis Distance, Minimum Distance, . . .), due to the fact that the latter are more restrictive and require assumptions about data distribution, which makes lithological mapping complicated in the study area, because each rock unit comprises a linear mixture on a microscopic scale of different minerals with a distinct spectral signature, which justifies their pixels' heterogeneity [48], [49]. Moreover, the high spatial and spectral resolution in the VNIR and SWIR bands of Sentinel-2A images [9], [15], allow to apply different spectral enhancement techniques, specifically Independent component analysis (IC1, IC3 and IC5) and two band ratios (BR), (band 4 + band 11)/(band 3 + band 8A) and (band 7 + band 11)/(band 8A + band 12), in order to extract all the rock units exposed in the study area and evaluate the capability of different classification techniques particularly, SVM-PBIA, SPBIA and SVM-GEOBIA, for generating the optimal lithological map with well-defined boundaries of the lithological units.

Despite the high potential of GEOBIA approach, a very limited number of research papers are available on its performance, specifically on Sentinel-2A imagery for discriminating lithological units. This study aimed to compare GEOBIA, SPBIA and PBIA classification approaches in lithological mapping; by using the most applicable MLA in geological mapping, which is the SVM algorithm [15] and focusing on a higher spatial and spectral dataset along with spectral enhancement processing to select the optimal technique for mapping rock features in a geologically complex semi-arid region. The results of this work, show that SVM-GEOBIA approach is predicted to be more efficient and surpass the

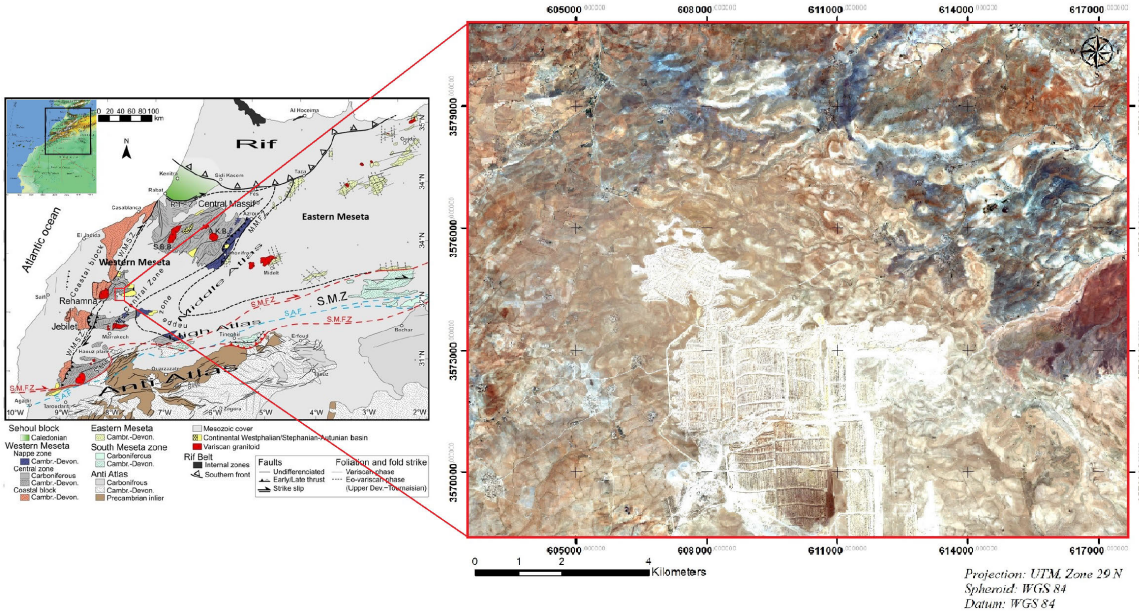

FIGURE 1. Study area (Google Earth imagery with resolution of 5m) on the simplified geological and structural map of the Moroccan Variscides [51].

other two approaches. The lithological maps obtained were then compared to the pre-existence geological map and validated by field investigation.

II. GEOGRAPHIC AND GEOLOGICAL SETTINGS OF THE STUDY AREA

The Skhour Rehamna Paleozoic massif of is a semi-arid region situated between the longitudes 7°54′55″ and 7°43′50″ west and the latitudes 32°22′30″ and 32°14′39″ north. It is a buttonhole located, as depicted in Figure 1, between the central Hercynian massif (Central Morocco) in the north and the Jebilet in the south [50].

The geological map used in this study is that of Skhour Rehamna (1/50 000), realized by the French government geological survey BRGM-CID (The geological and mining research bureau), and published in 2004 by the Ministry of Industry, Trade, Energy and Mines of Morocco [50] (Figure 2). It consists primarily of lower metamorphic rocks formed by two major units, as described below:

The Ouled Hassine Devonian entity [52] that is predominantly with micashists, that are marked by the presence of reference levels composed of a combination of carbonate bars, quartzite bars and more rarely conglomerate levels [53]. The Unit of Lalla Tittaf [54] which the age remained until now as Visean, although it may be in the Paleoproterozoic age [53]. The contact between the micaschists of the Lalla Tittaf Unit and those of the Ouled Hassine Unit are not visually marked in the ground. However, the distinction between the two units is generally based on their composition: Lalla Tittaf presenting various orthoderivated rocks (lenses of amphibolites, porphyroids and gabbroic bodies) and small carbonate levels containing semipelites and metapelites of metabasite, orthogneiss, calcschist, and marble intercalations [52], which make this unit darker than Ouled Hassine Unit [50], [53].

Moreover, The Dalaat el Kahlat entity, whose age remains uncertain, lies between the two units. It is characterized by the same facies as the Unit of Ouled Hassine with predominance of micaschists that is marked by a combination of carbonate bars, quartzite bars and more rarely conglomerate levels [55]. Also, in the NW of the geological map of the study area outcrops the granite of Ras el Abiod that is broadly arenized [50].

The south side of the geological map, is covered by the phosphate series which constitutes the eastern part of the Maastrichtian Gantour deposit, it is mined at Ben Guerir, in a very large surface [50].

III. MATERIALS AND METHODS

A. DATASETS AND PRE-PROCESSING

The Sentinel-2A cloud-free imagery used in this study was acquired on 29 October 2017. The software package of the platform developed by the ESA (SNAP) was used for atmospheric and terrain correction of the Sentinel-2A Top-Of-Atmosphere (TOA) Level-1C image. The Sentinel-2A Level 2A BOA orthorectified reflectance image was generated using the ESA Sen2Cor processor (version 2.3.1) [56], [57]. The processing includes optional cirrus correction, terrain correction in addition to the retrieval of Aerosol optical Thickness (AOT) and Water Vapor (WV) content [57]. Sen2Cor relies on the Digital Elevation Model (DEM) that is downloaded automatically by the processor SRTM (Shuttle Radar Topography Mission Digital Elevation Model) in order to achieve a Bottom-Of-Atmosphere (BOA) corrected reflectance orthoimage. In this research, the default parameters in Sen2Cor were used, ignoring Cirrus correction and

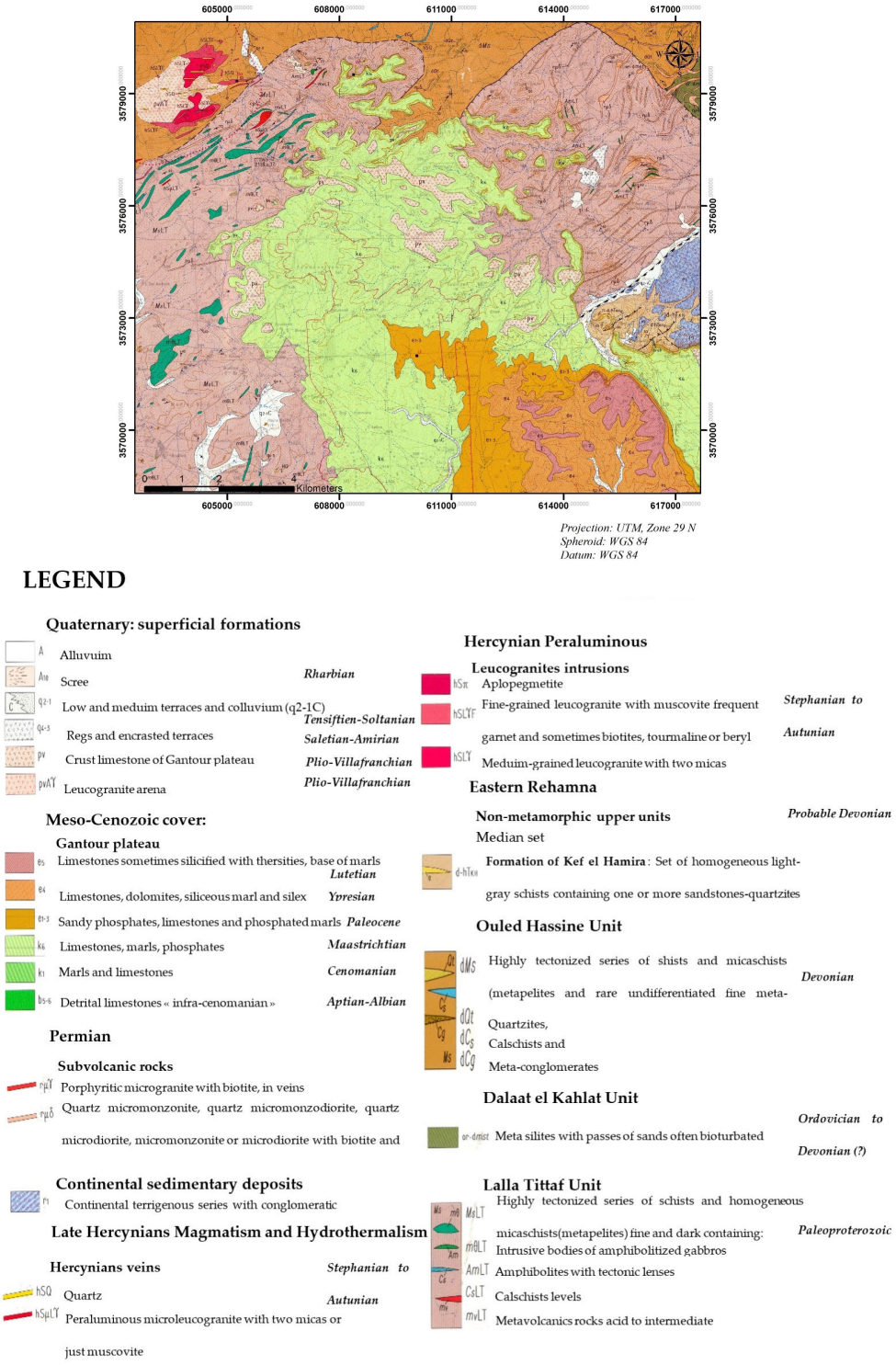

FIGURE 2. **Extract of Skhour Rehamna Geological map 1/50 000 (Realized and published by the group BRGM-CID in 2004) ©.**

WV retrieval. In the present research, spectral bands 1, 9 and 10 were removed due to the sensitivity to clouds, aerosol in addition to the low spatial resolution (60m) (Table 1) [58]. The remaining 20 m spatial resolution bands were resampled to 10 m modifying the pixel spacing to match the VNIR bands resolution. The datasets were finally re-projected in the WGS84 coordinate system and UTM projection i.e. zone 29N.

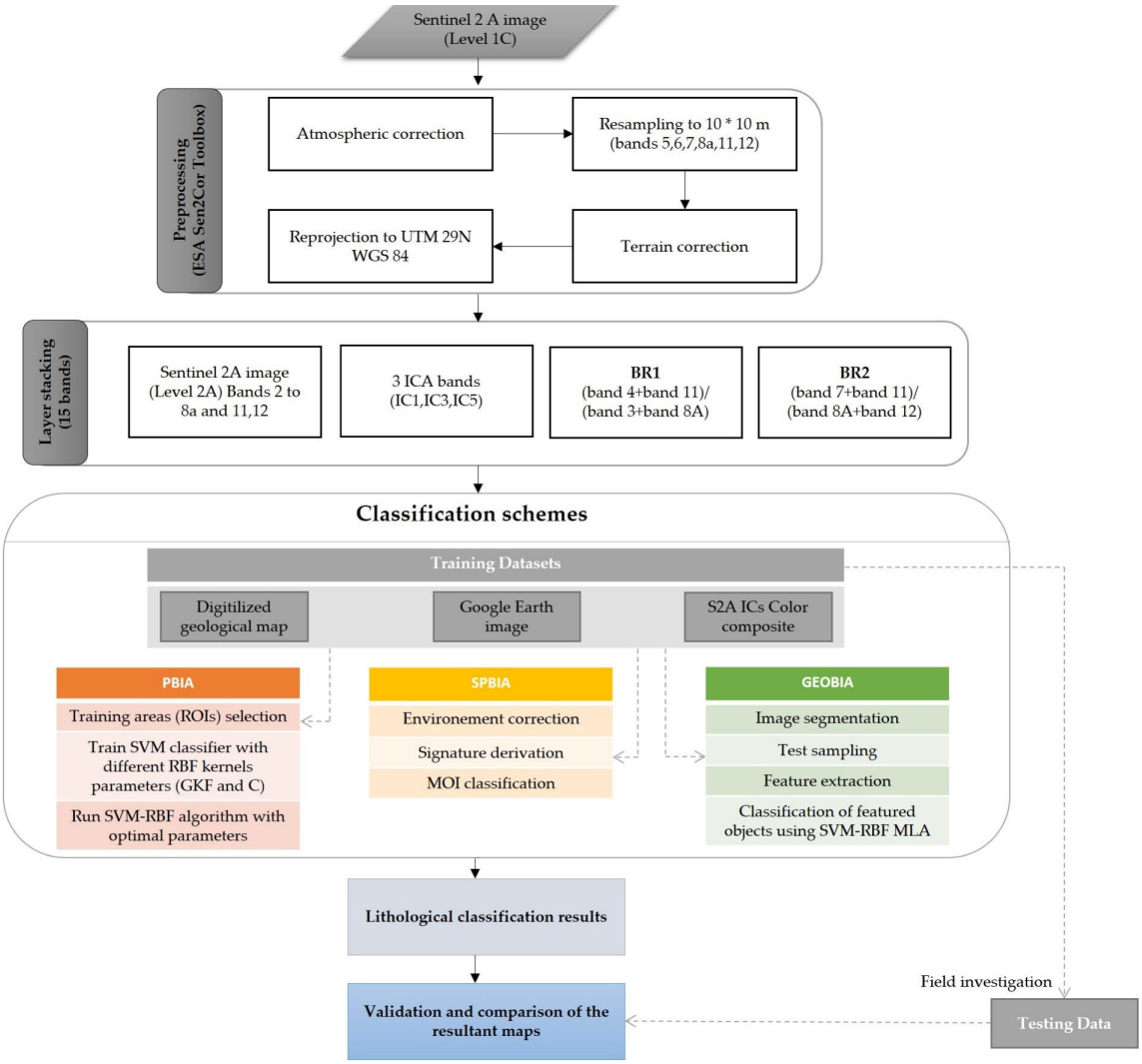

FIGURE 3. General workflow of the methods.

B. PROCESSING

The sentinel-2A image bands were layer stacked to the three Independent Component bands (IC1, IC3 and IC5) and two band ratios (BR) due to its high discrimination of the rock types exposed in the study area. An overview of the methods used in this research is shown in Figure 3.

1) BAND RATIO (BR)

Band ratioing is a spectral enhancement technique broadly used in lithological discrimination [4], [59], [60], due to its proven ability to highlight rock-units that cannot be distinguished apparently in the raw bands, by dividing the reflectance value of each pixel in one image band by the value of reflectance in the pixel of the other band [61]. This technique is efficient in minimizing shadow effects owing to topography. Spectral signature provides helpful hints for settling on the bands employed for ratioing, where target earth surface material will appear as bright or dark pixel in the BR image. Different band ratios for mineral and rock detection have been developed based on the spectral absorption and reflectance properties of rocks and minerals. for example, Khan *et al.* (2007), employed ETM + band ratios of 5/7, 4/5, and 3/1 to delineate mafic and ultramafic rocks [62]. Pournamdari *et al.* (2014b) created a false color composite for lithological differentiation in an ophiolite complex using specific ASTER band ratios of 4/7, 4/5, and 4/1 [63]. Wenyan Ge *et al.* (2018) used Sentinel-2A and Aster datasets to extract band ratio, (S3 + A9)/(S12 + A8), to discriminate the serpentine in the ophiolite complex [4]. In this study, the spectral signature extracted from S2A imagery, which is characterized by the highest reflectance, of all lithologies exposed in the study area, at band 7 and band 11, against the highest absorption in band 12 and band 8A, in addition to the first reflectance of all facies at band 3 against the absorption at band 4 (Figure 4), which leads to use the two most effective and accurate band ratios, (band 4 + band 11)/

TABLE 1. Spectral bands characteristics of Sentinel-2A MSI.

Band Number	Spectral Characteristic	Central wavelength (nm)	Spatial resolution (m)
B1	Coastal aerosol	443	60
B2	Blue (B)	490	10
B3	Green (G)	560	10
B4	Red (R)	665	10
B5	Vegetation red edge 1 (Re1)	705	20
B6	Vegetation red edge 2 (Re2)	740	20
B7	Vegetation red edge 3 (Re3)	783	20
B8	Near infrared (NIR)	842	10
B8a	Near infrared narrow (NIRn)	865	20
B9	Water Vapor	945	60
B10	Shortwave infrared Cirrus	1380	60
B11	Shortwave infrared 1 (SWIR1)	1910	20
B12	Shortwave infrared 2 (SWIR2)	2190	20

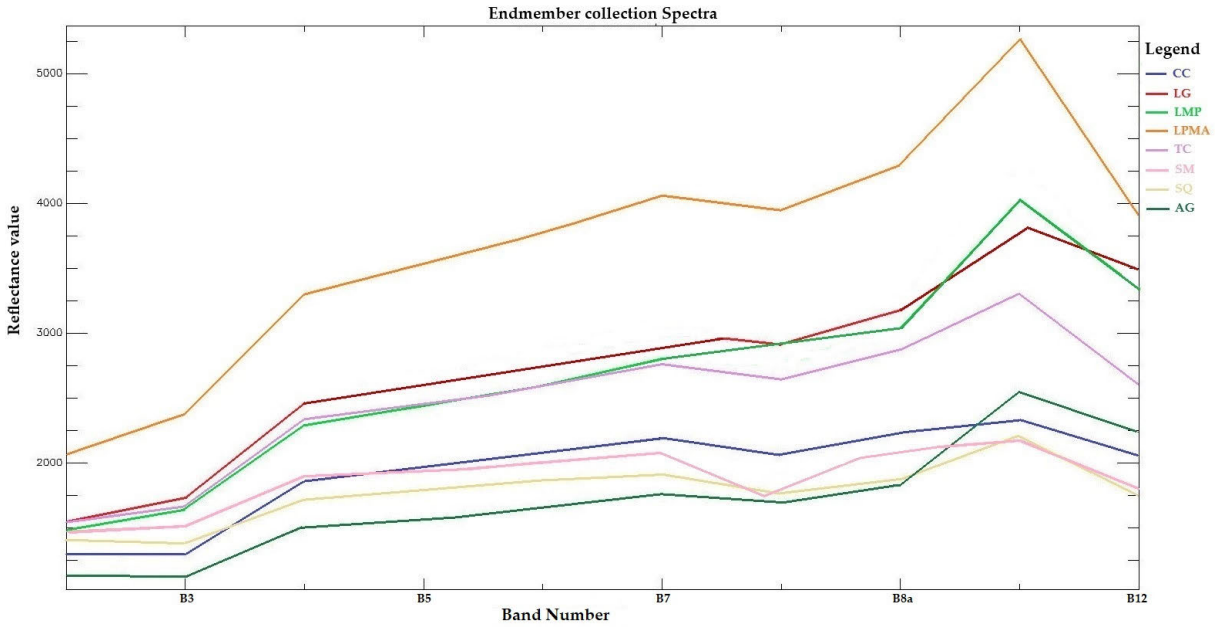

FIGURE 4. Spectral characteristics of lithological units exposed in the study area using S2A spectral bands.

(band 3 + band 8A) and (band 7 + band 11)/(band 8A + band 12), BR1 and BR2 (Figure 5) respectively, in order to highlight all the rock units exposed in the region of interest.

2) INDEPENDENT COMPONENT ANALYSIS (ICA)

Independent component analysis (ICA) is a statistical and high order computational feature extraction technique, it can be applied on multispectral or hyperspectral remote sensing datasets, in order to expose hidden factors behind random variable sets, signals or measures [64], [65]. This transform consists of finding maximally independent and non-gaussian components [66], [67]. Moreover, the output independent component (IC) are not only uncorrelated, as principal component analysis (PCA), but also independent and containing features details even when they cover just a small portion of image pixels [68]. ICA transformation can be used for image characteristics extraction, noise reduction, feature separation, endmember extraction, target and anomaly identification, classification and mapping.

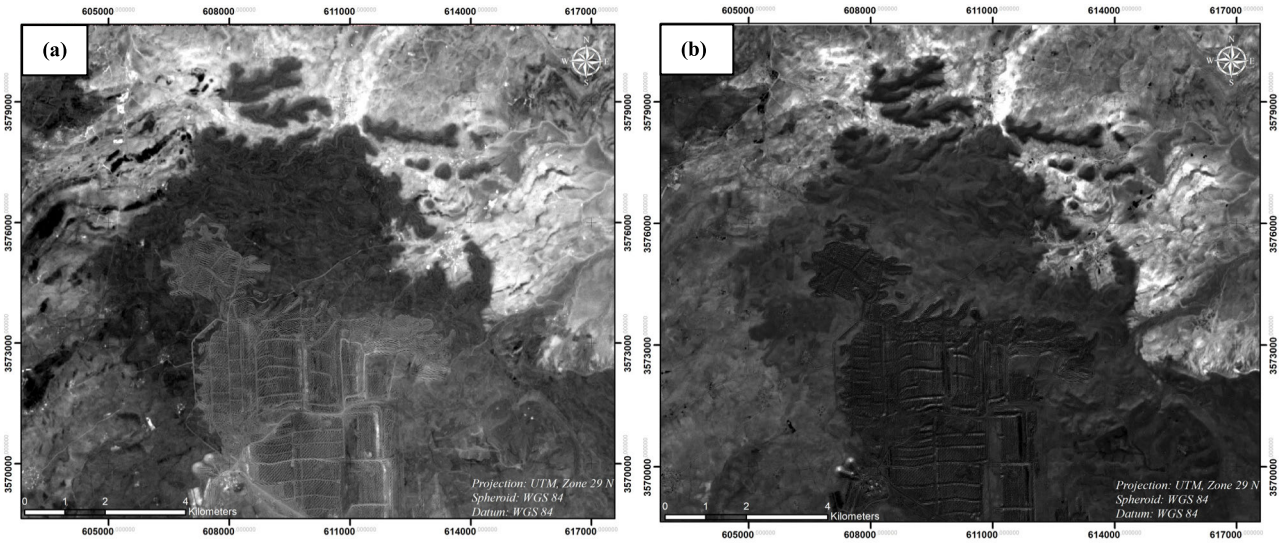

FIGURE 5. Band Ratios extracted from S2A imagery: (a) BR1 and (b) BR2.

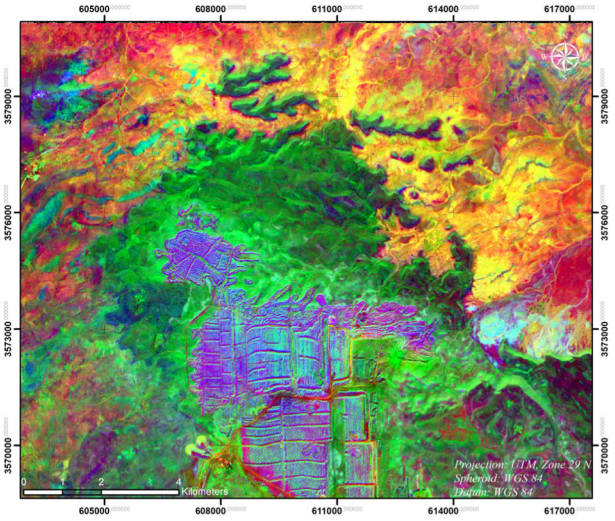

FIGURE 6. The Sentinel-2A ICs (1, 3, and 5) combination.

A visual interpretation of the resulted IC bands had led to choose the IC1, IC3 and IC5 (Figure 6) for their interpretable RGB color composite that successfully enable us with the help of geological map and field investigation to extract all ROIs of the lithologies exposed in the investigated region.

3) SUPPORT VECTOR MACHINE CLASSIFICATION ALGORITHM

Special interest has recently been focused on Support Vector Machines (SVM) as a superior supervised MLA, increasingly applied for geological mapping [47], [69]–[71]. SVM is a statistical non-parametric learning method which was defined by Vapnik and Chervonenkis [72]. By focusing on the training samples (Support Vectors) [73], which are placed at the margin of class descriptors [74], the SVM classification approach aims to find the optimum separating hyperplane between classes (Figure 7).

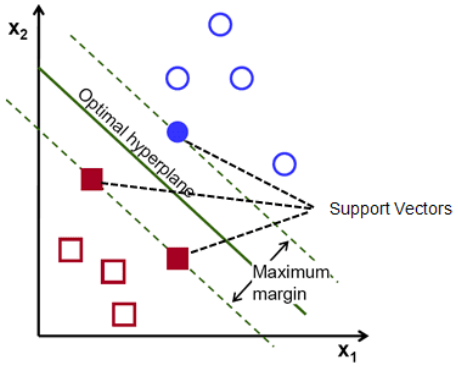

FIGURE 7. Representation of the hyperplane, the support vectors and margin [75].

In the SVM algorithm, there are four kernel functions developed: linear, polynomial, sigmoid and Radial Basis Function (RBF). SVM-RBF was applied in this study because it classify the given support vectors non-linearly into a larger dimensional feature space [76]. The GFK parameter specifies how far the influence of a single training example reaches, as long as the C parameter controls the trade-off between the misclassification on the training data and the simplicity of the decision boundary. The high performance of the SVM, using RBF kernel, classification accuracies depends on the right choice of regions of interest (ROIs) and the training parameters particularly, Gamma Kernel Function (GKF) and the penalty parameter [77], the most accurate prediction was attained using error penalty value ($C = 100$), and a GKF equaling to 0.1. We tested SVM RBF algorithm for both PBIA and GEOBIA approach for comparison.

4) PBIA

The PBIA approach focus on assigning any pixel to the surrounding pixels by taking into account each pixel's spectral properties and ignoring contextual characteristics [78]–[80].

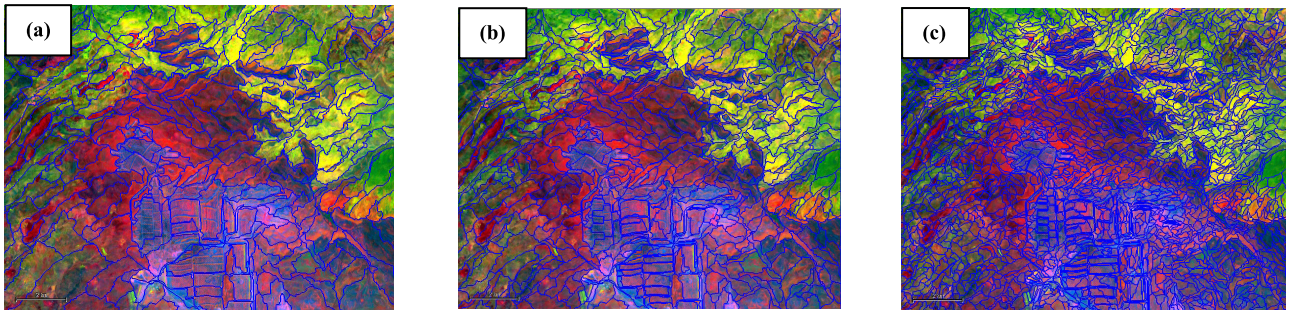

FIGURE 8. The segmentation result for different scale parameter values: (a) 9; (b) 6; and (c) 3 the blue lines show the boundaries of the extracted objects superposed on the RGB color composite generated with the IC3, BR2, B2 bands.

In this study, SVM (RBF) algorithm was implemented,, as it is the most effective and applicable MLA in the field of geological mapping [15], [59], [81].

5) SPBIA

SPBIA technique is used to address the major limitation of PBIA classification approach connected with mixed pixels since they can assign pixels a degree of membership to many classes, as it is wildly used in geological and mineral mapping [82]–[84].

A variation of both pure and mixed pixels is also found in remotely sensed datasets. Mixed pixels are assigned to the class with the greatest proportion of coverage or likelihood through complicated classification techniques. During this process, data loss is unavoidable. In order to correct this loss, soft classification methods were introduced: they allocate pixel fractions to the earth's surface classes corresponding to the represented region within a pixel [85].

This is the principal of SPBIA approach that has been developed to detect materials that are smaller than the size of the image pixel, to improve the classification accuracy. It consists of discriminating between different classes within the spectrum of the single pixel, and reducing problems associated with mixed pixels [86].

Subpixel classification is based on four principal sequential components [87]:

–Preprocessing

It is a required prior step that consist of removing the background spectra of the image and leave only the Material of Interest (MOI) candidate spectrum.

–Environment correction

An automatic necessary process, that calculate a set of environmental correction factors to prepare the image for signature derivation.

–Signature derivation

The signature derivation function is a required step that allows to develop a signature for a particular MOI to classify an image.

–MOI classification

It is the final stage in sub-pixel classification; it consists of finding the pixels that contain spectral properties similar to the given MOIs signature.

6) GEOBIA

The process of producing a generalized lithological map from a set of abundance maps in SPBIA approach is rather subjective and frequently necessitates further visual interpretation of lithological boundaries [88]. which led to use GEOBIA approach that is generally capable of eliminating the ''salt-and-pepper'' artefact and mapping lithological contacts more accurately.

GEOBIA approach is an effective technique to delineate several image objects arranged by their relative resemblances in spectral, spatial and textural properties in an integrative way [89]. The GEOBIA approach offers a procedural framework using two main phases [90]:

–Image segmentation is recognized as the initial and the crucial step in GEOBIA approach [91]. It consists of dividing the image into neighboring pixels with similar characteristics that are based on spatial, textural and relational information that define the homogeneity of the resultant object [92]. In this study, segmentation was accomplished using the multiresolution image segmentation (MRS) algorithm (Figure 8). This algorithm starts with each pixel region and consecutively group them into meaningful objects, based on homogeneity criterion [28]. The necessary prerequisite for a successful MRS is the optimization of the following parameters:

- The scale parameter (SP), defined also as homogeneity criteria. This criterion is considered as the most critical of MRS process as it controls the homogeneity and the image object size. Therefore, higher the SP, bigger and more merging are the objects, and vice versa [90], [93]. SP was selected visually using ''trial-and-error'' approach, by evaluating the segments obtained using different fixed scale values (Figure 8). This medium scale parameter of 6 (Figure 8.b) was preferred to perform the image segmentation, because it conserved the spatial information and avoids under-segmentations that results heterogeneous image objects.
- The shape or the color criterion, can be considered as pixels spectral values heterogeneity of the objects formed. If the weight of the shape factor is high, then the influence of the image color decrease in the segmentation, and vice versa [90].

TABLE 2. Parameter values used for multi-resolution image segmentation.

Parameters	Value
Scale	6
Shape	0.01
Compactness	0.08

- The smoothness or compactness criteria affect the shape between compact edges and smooth boundaries [90]. A high weighted compactness will lead to more compact objects and smoother boundaries.

In addition to the different weighting of the 15 input layers, those parameters must be as accurate as possible to obtain meaningful and real-world objects. The parameter values used to perform the multi-resolution image segmentation are shown in Table 2.

–Feature extraction and classification, is the second and last stage in GEOBIA approach. It sought to select a set of feature vector to differentiate between the target classes and create connectivity between real-world classes and the image objects to apply a suitable classification rule. In this study, the classification of image objects was carried out by SVM classifier.

7) ACCURACY ASSESSMENT

In order to evaluate the accuracy of the classified images generated from different classifiers, the confusion matrix was carried out, comparing the results to the pre-existing geological map of the research region, by computing the statistical accuracies for each result obtained using a sample plots of validation pixels [94]. The Kappa coefficient (K) is an appropriate accuracy measure between thematic maps and reference data, it takes into account the entire elements of the confusion matrix (diagonal and non-diagonal). The overall accuracy (OA) takes into consideration just the diagonal elements of the confusion matrix. Two other thematic errors, take into account the accuracy of each class individually, were used. One is provided by the producer's accuracy (PA), which identifies the proportion of a ground image pixel correctly labeled by the classifier. The second error is presented by user's accuracy (UA), which indicates the probability that a classified pixel from the resultant map is in fact that lithology on the ground [94]. Also, the reference data based on the field work outcrops, with several GPS points that was held on 26 October 2019, were used to validate the resultant maps.

IV. RESULTS

The results of the lithological maps, generated from the subpixel in addition to both pixel-based and object-based approaches using SVM algorithm are described in the following sub-sections.

A total of eight general litho-classes are identified (Figure 9.a): Limestones, marls, phosphates (LMP), intrusive bodies of Amphibolitized Gabbro (AG), Set of homogeneous light-gray schists containing one or more sandstones quartzites bars very tectonized (SQ), Continental terrigenous series with conglomeratic dominance (CC), Low and medium terraces and colluvium (TC), Limit of the phosphates mining area (LPMA), Schists and mica schists (SM), and Leucogranite (LG).

Although all the approaches generated aggregations of lithologies exposed in the field of research, the most prominent difference between the thematic maps classified by the PBIA, SPBIA and GEOBIA methods, from visual inspections, is that: the lithological map obtained using PBIA SVM machine learning algorithm give more speckled regions than the other lithological maps, as shown in the Figure 9.b. Thus the classification results of low and medium terraces and colluvium (TC), limestones, marls, phosphates (LMP) and the leucogranite (LG) marked by the blue, the yellow and the red circles, respectively, are largely misclassified into surrounding lithological units. In addition, as illustrated by the orange circle, the Continental Terrigenous series with conglomeratic dominance (CC) is completely misclassified into Schists and mica schists using per-pixel approach.

Since the SPBIA approach was developed to overcome the challenge of mixed pixels, the fractional abundance images for each litho-class have been shown in the Figure 10. Also, it is clear in Figure 9.c that this process enabled the detection of some facies such as Limestones, marls, phosphates and the schists and mica schists, illustrated by the yellow and green circles respectively, that were mixed in PBIA method. Otherwise, abrupt appearance could be seen in the SPBIA approach, due to the shadow effect, compared to the GEOBIA method resultant map (Figure 9.d) that is more efficient, reduce the salt and pepper effect and give a better visualization with more pronounced boundaries compared to the other two approaches as it takes into consideration the shape of features and this can be illustrated by the Continental terrigenous series with conglomeratic dominance (CC), the leucogranite and Low and medium terraces and colluvium (TC), marked by the orange, red and blue circles accordingly, that was identified very well by this method.

This distinction can be due to the fact that the characteristics of the GEOBIA are composed of multi-pixel units and have been classified as such, while the PBIA were classified as per-pixel level based on spectral characteristics only.

V. DISCUSSION AND VALIDATION

Satellite borne remote sensing images are increasingly becoming more available, thus making them an important resource to geological mapping. The traditional methods have been proven to be time and cost-intensive, making it difficult to completely utilize these useful datasets [15]. Although the methods of PBIA classification can provide adequate results for lithological mapping over semi-arid areas, there have been some limitations, found in their ability to generate detailed geological maps, related to the topographic effect and solar illumination variations that caused the mixed pixels.

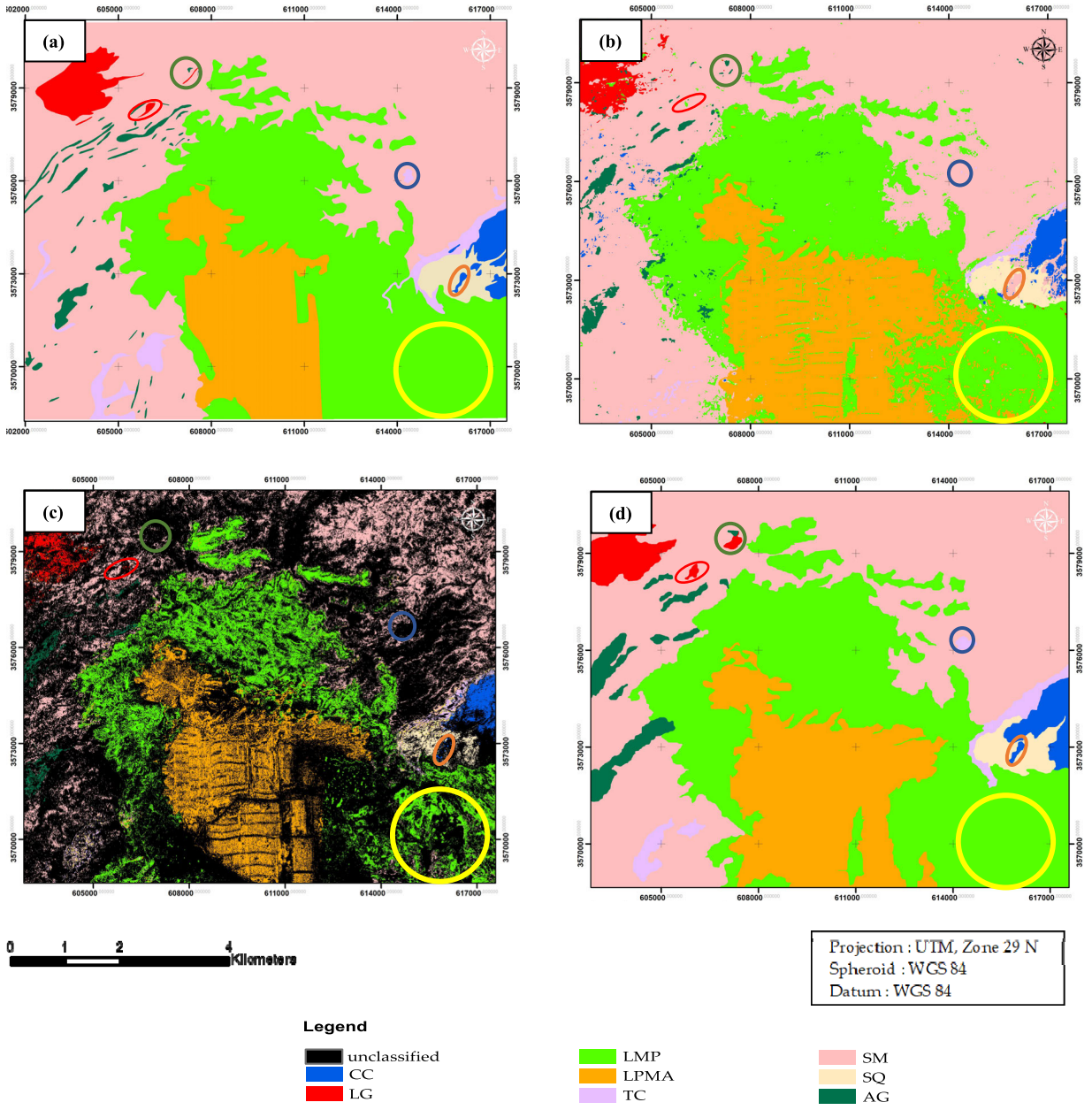

FIGURE 9. (a) Digitalized geological map; Thematic map results of (b) PBIA-SVM, (c) SPBIA and (d) GEOBIA-SVM classification methods.

Figure 9.b represents the example of mixed litho-classes, e.g., between low and medium terraces and colluvium (TC) and schists and mica schists (SM) which is marked by a blue circle in SVM PBIA approach. In addition to the salt and pepper problems, as shown by the yellow circle in Figure 9.b, which are occurred due to the use of only image pixel spectral information. In order to overcome the problems associated with mixed pixels, SPBIA classification technique was applied. However, the incoherency of SPBIA resultant lithological map caused by the shadow effect (Figure 9.c), as well as the high spatial resolution of Sentinel-2A imagery led to the emergence of GEOBIA classification approach, that performs by taking into account not only spectral characteristics but also the texture, spatial and geometry of features during the process of classification [95].

The use of parametric classifiers for mapping complicated spectral heterogeneous regions was discouraged due to the fact that they employ the assumptions normality between the provided training dataset [93]. Nevertheless, the use of non-parametric MLAs such as, Neural Networks (NN), Random Forest (RF) and Support Vector Machines (SVM) is recommended because they do not use any presumptions regarding the statistical relationship between the training dataset presented and can also allow the inclusion of auxiliary data that may be essential in enhancing accuracy assessment [96], [97].

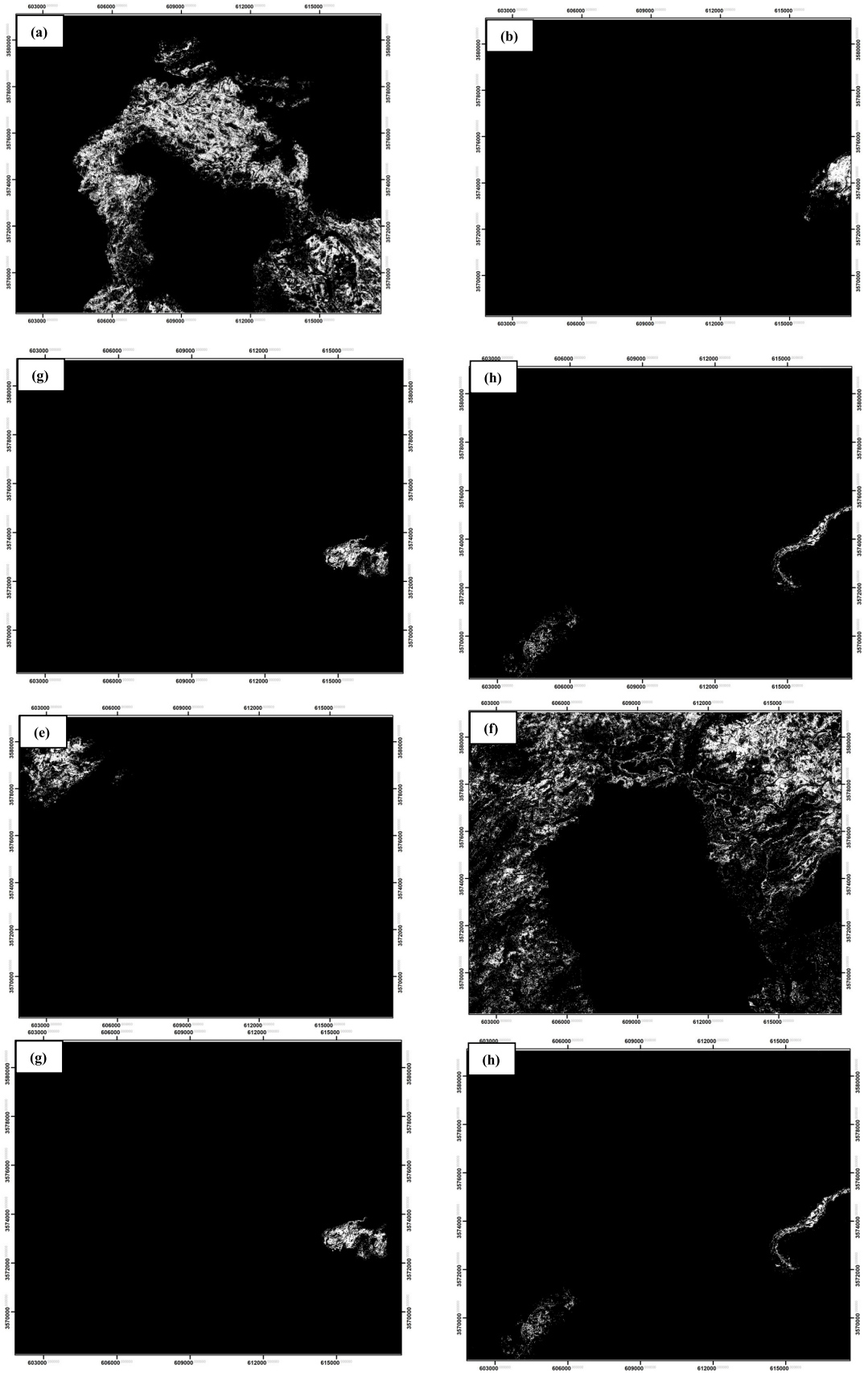

FIGURE 10. The fraction images of classes from the subpixel classification (a) LMP (b) CC (c) LPMA (d) AG (e) LG (f) SM (g) SQ (h) LC.

TABLE 3. Synthesis of accuracy results for the different classifiers.

	Statistics	Average Kappa indices	Standard deviation of Kappa indices	Average Overall Accuracy (%)	p-Value
Classification approaches	PBIA	0.80	0.053	87	<0.0001
	SPBIA	0.84	0.076	89	<0.0001
	GEOBIA	0.89	0.046	93	<0.0001

In this study, SVM PBIA, SPBIA and SVM GEOBIA approaches were compared and evaluated in terms of mapping lithological units in semi-arid regions such as the southern of the western Moroccan Meseta, by integrating Sentinel-2A spectral enhancement techniques, particularly the two BR and ICs bands (1, 3 and 5) in order to improve lithological mapping.

A. STATISTICAL COMPARISON OF RESULTANT MAPS

Accuracy assessment was performed for the above three techniques using random sampling technique, in which 33 trials of around 1000 random samples were distributed in the study area. Besides the digitalized geological map of the region of study was used as a reference image to analyze the accuracy results. Table 3 presents the average overall accuracy (OA), as well as the average kappa indices (K) their standard deviation and the statistical significance of differences (p-value) between the GEOBIA, SPBIA and PBIA approaches. Therefore, the statistical comparison between the three classification methods demonstrated that the GEOBIA approach outperforms its PBIA and SPBIA counterparts ($p < 0.0001$), with an average kappa difference of 5% and 9% in SPBIA and PBIA, respectively (Table 3) and show smoother lithological map. This is most likely because the integration of spatial and spectral information into the classification process of GEOBIA method as well as combining the values of all contiguous pixels within objects which reduces the intra class variability that is identified as heterogeneous pixels when they are considered individually in pixel-based approaches. The PBIA approach gave less accuracy due to the salt and pepper effects, otherwise the SPBIA method exceeded the accuracy of its per-pixel equivalent, but it underperforms its GEOBIA counterparts due to the shadow effect.

Through the comparison of the resultant lithological maps using different approaches, it can be concluded that GEOBIA SVM classification surpassed the accuracy statistics with the PBIA and SPBIA classification methods falling short (Table 3), moreover, the lithological maps generated from SVM GEOBIA (Figure 9.d) approach provided close depictions of the broad rock-units in the geological map of the study area, by reducing the salt-and-pepper artifacts and producing smoother features with well-defined limits between litho-classes.

Even though, SVM GEOBIA approach improved the accuracy of lithological maps and outperforms those produced by the other two classifiers with regards to OA and K. The performance of classifying the individual litho-classes is slightly

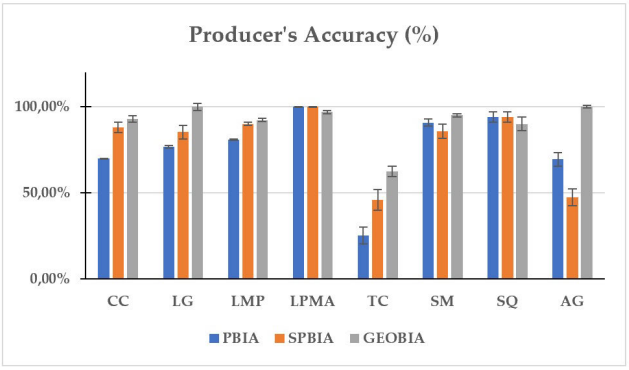

(a)

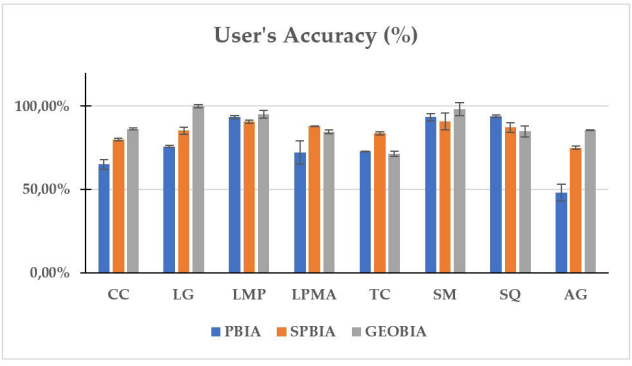

(b)

FIGURE 11. Average accuracies and standard deviation of the individual lithological classes: (a) PA; and (b) UA.

different between the methods, as it's graphically demonstrated in Figure 11. For instance, despite the greatest OA and K of SVM GEOBIA approach, its PA and UA are lower than the other two approaches for some lithological classes (e.g., LPMA and SQ). Such variation may indicate that a single scale value is insufficient for segmenting all lithological units [98]. Generally, when each type of classifier is considered individually, the overall superiority of the GEOBIA approach over PBIA and SPBIA approaches is usually attributed to improve discrimination of lithological units with low intra-class variability (e.g. CC, LMP, LG, SM and AG), Because those rock-units are homogeneous and particularly distinctive in terms of topography. The observed increases in PA and UA of GEOBIA over the PBIA and SPBIA approaches are most usually related to the averaging effect, which leads to a decrease in intra-class heterogeneity, improved distinction between classes, reduce "salt-and-pepper" artefact and eliminate shadow

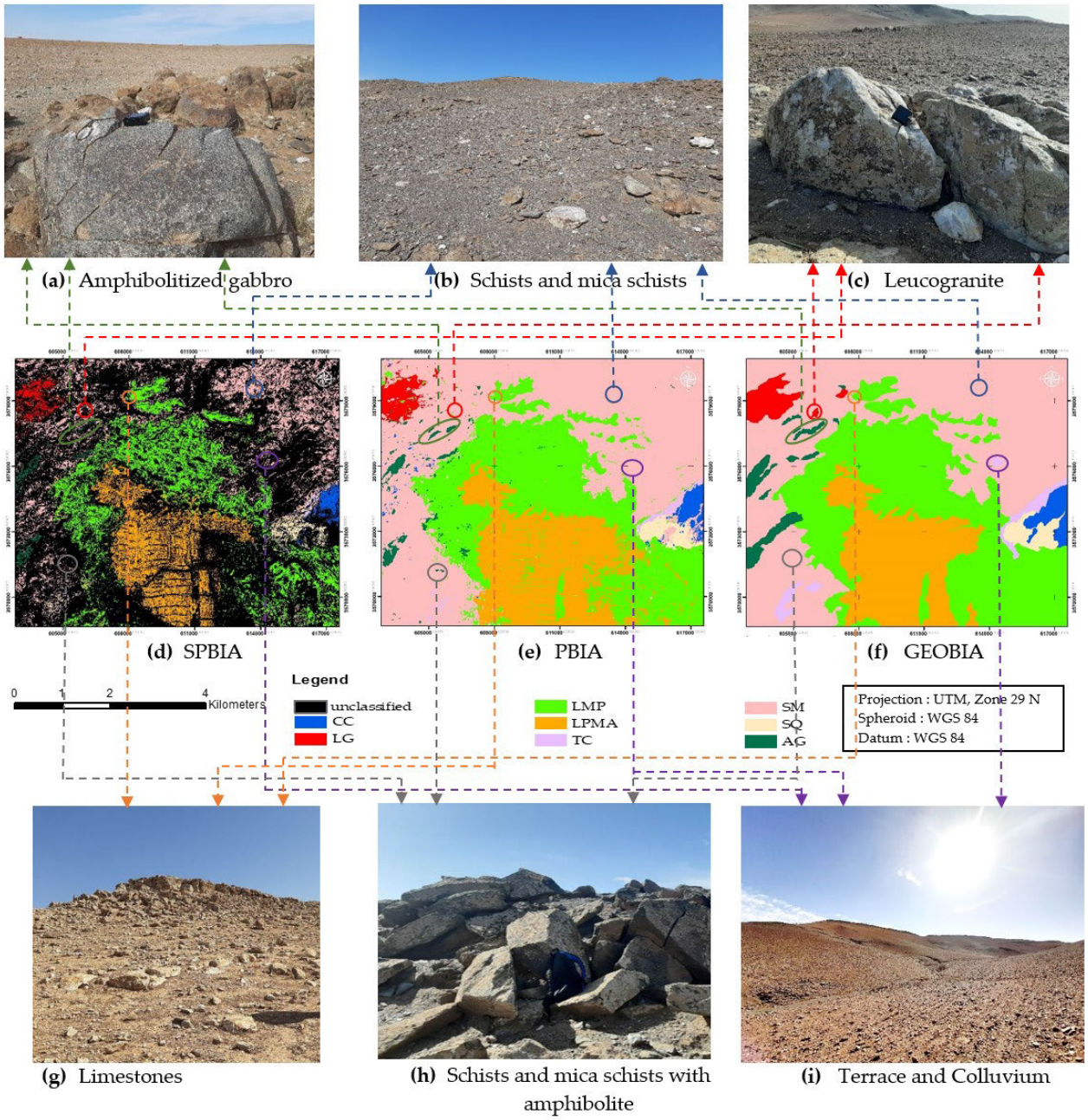

FIGURE 12. Field photographs showing different lithological units of study area and their respective localization in the resultant maps: (a) Amphibolitized gabbro; (b) Leucogranite; (f) Limestones; (g) Schists and mica schists with amphibolite.

effect, which confirm the key reason for choosing GEOBIA over PBIA and SPBIA approaches for lithological mapping in complex semi-arid regions. Irrespective of the classification approaches, meaningful and efficient PA and UA accuracies obtained over heterogeneous lithological units are usually low (e.g. TC and AG), whereas high accuracy estimates are obtained over homogeneous regions.

B. FIELD VALIDATION

After the comparison of the results with the previous geological map, a validation with field investigations was performed, by identifying classes of the lithological maps produced using the three approaches with their respective rocks exposure in the study area (Figure 12). The lithological units of the SIX field locations are somewhat agreed with the predicted litho-classes in the lithological maps generated from SVM GEOBIA and SPBIA approaches, it has also been observed that the PBIA method didn't show some facies such as the small outcrop of leucogranite (LG) and the Amphibolitized Gabbro (AG), nevertheless the amphibolite in the schist and mica schist in the south of the study area is well identified using SVM PBIA approach. However, it has been recognized

that the previous geological map of the study area shows considerable compatibility with ground existence.

In summary, the integration of high spatio-spectral resolution datasets along with spectral enhancement techniques and SVM GEOBIA approach, can be utilized for recognizing rock outcrops and generating precise, homogeneous lithological maps with well-defined boundaries of litho-units, in heterogeneous semi-arid regions.

VI. CONCLUSION AND FUTURE DIRECTIONS

Selecting the best classifier is essential in determining geological units. Consequently, this study assesses the efficacy and prospects the originality of the SVM machine learning algorithm in pixel and object-based classification approaches to improve the discrimination of lithologies by comparing them to SPBIA method, in addition to the added value of integrating the spectral information contained in the neochannels extracted from Sentinel-2A imagery, including BR and ICA. Besides, the three major techniques have been validated and confirmed through the geological map and series of field investigations. The results showed that the GEOBIA method gave a higher overall accuracy and larger kappa coefficient, following by the SPBIA classifier and the PBIA approach results the lowest accuracies. The visual comparison also highlighted the importance of the segmentation step by showing that the classification of homogenous objects reduces the heterogeneity of classes caused by shadow and salt and pepper artefacts, therefore producing a greater classification accuracy. Though the results obtained from the three algorithms, all approaches have some pros and cons. Thus, our new research will be based on finding appropriate algorithms by executing a hybrid method, which can accurately discriminate individual litho-classes exposed in the ground using the cloud computing to produce an optimal geological map of all the region of Rehamna.

ACKNOWLEDGMENT

The authors would like to thank the ESA Sentinels Scientific Data Hub for MSI and SNAP Platform and BRGM-CID for the geological map.

AUTHOR CONTRIBUTIONS

Conceptualization, Imane Serbouti, Mohammed Raji, Mustapha Hakdaoui, Biswajeet Pradhan; methodology, Imane Serbouti, Mohammed Raji, Mustapha Hakdaoui Biswajeet Pradhan; software, Imane Serbouti, and Mustapha Hakdaoui; validation with field investigations, Imane Serbouti and Mohammed Raji; writing original draft preparation, Imane Serbouti; review and editing, Biswajeet Pradhan, Chang-Wook Lee, and Abdullah M. Alamri; supervision, Mohammed Raji, Mustapha Hakdaoui, and Biswajeet Pradhan; and funding acquisition, Biswajeet Pradhan, Chang-Wook Lee, and Abdullah M. Alamri.

CONFLICT OF INTEREST

The authors declare no conflict of interest.

REFERENCES

[1] Z. Adiri, R. Lhissou, A. El Harti, A. Jellouli, and M. Chakouri, "Recent advances in the use of public domain satellite imagery for mineral exploration: A review of Landsat-8 and Sentinel-2 applications," *Ore Geol. Rev.*, vol. 117, Feb. 2020, Art. no. 103332, doi: 10.1016/j.oregeorev.2020.103332.

[2] M. Pal, T. Rasmussen, and A. Porwal, "Optimized lithological mapping from multispectral and hyperspectral remote sensing images using fused multi-classifiers," *Remote Sens.*, vol. 12, no. 1, p. 177, Jan. 2020, doi: 10.3390/rs12010177.

[3] D. Nemmour-Zekiri and F. Oulebsir, "Application of remote sensing techniques in lithologic mapping of Djanet Region, Eastern Hoggar Shield, Algeria," *Arabian J. Geosci.*, vol. 13, no. 14, pp. 1–10, Jul. 2020, doi: 10.1007/s12517-020-05648-5.

[4] W. Ge, Q. Cheng, L. Jing, C. Armenakis, and H. Ding, "Lithological discrimination using ASTER and Sentinel-2A in the Shibanjing ophiolite complex of Beishan orogenic in Inner Mongolia, China," *Adv. Space Res.*, vol. 62, no. 7, pp. 1702–1716, Oct. 2018, doi: 10.1016/j.asr.2018.06.036.

[5] F. Masoumi, T. Eslamkish, A. A. Abkar, M. Honarmand, and J. R. Harris, "Integration of spectral, thermal, and textural features of ASTER data using random forests classification for lithological mapping," *J. Afr. Earth Sci.*, vol. 129, pp. 445–457, May 2017, doi: 10.1016/j.jafrearsci.2017.01.028.

[6] X. Zhang and P. Li, "Lithological mapping from hyperspectral data by improved use of spectral angle mapper," *Int. J. Appl. Earth Observ. Geoinf.*, vol. 31, pp. 95–109, Sep. 2014, doi: 10.1016/j.jag.2014.03.007.

[7] H. van der Werff and F. van der Meer, "Sentinel-2 for mapping iron absorption feature parameters," *Remote Sens.*, vol. 7, no. 10, pp. 12635–12653, Sep. 2015, doi: 10.3390/rs71012635.

[8] Y. Murayama and M. Ranagalage, "Remote sensing Sentinel-2 data for land cover/use mapping: A review," *Remote Sens.*, vol. 2291, no. 12, p. 14, 2020.

[9] F. D. Van der Meer, H. M. A. Van der Werff, and F. J. A. Van Ruitenbeek, "Potential of ESA'S Sentinel-2 for geological applications," *Remote Sens. Environ.*, vol. 148, pp. 124–133, Apr. 2014, doi: 10.1016/j.rse.2014.03.022.

[10] P. Blaschke, T. Lang, S. Lorup, E. Strobl, and J. Zeil, "Object-oriented image processing in an integrated GIS/remote sensing environment and perspectives for environmental applications. Environmental information for planning, politics and the public," *Environ. Inf. Planning, Polit. Public*, vol. 2, pp. 555–570, Jan. 2000.

[11] S. Asadzadeh and C. R. de Souza Filho, "A review on spectral processing methods for geological remote sensing," *Int. J. Appl. Earth Observ. GeoInf.*, vol. 47, pp. 69–90, May 2016, doi: 10.1016/j.jag.2015.12.004.

[12] F. D. van der Meer, H. M. Van der Werff, F. J. Van Ruitenbeek, C. A. Hecker, W. H. Bakker, M. F. Noomen, M. Van Der Meijde, E. J. M. Carranza, J. B. De Smeth, and T. Woldai, "Multi- and hyperspectral geologic remote sensing: A review," *Int. J. Appl. Earth Observ. Geoinf.*, vol. 14, pp. 112–128, Feb. 2012, doi: 10.1016/j.jag.2011.08.002.

[13] K. Fatima, M. U. K. Khattak, A. B. Kausar, M. Toqeer, N. Haider, and A. U. Rehman, "Minerals identification and mapping using ASTER satellite image," *J. Appl. Remote Sens.*, vol. 11, no. 4, Oct. 2017, Art. no. 046006, doi: 10.1117/1.jrs.11.046006.

[14] Z. Adiri, A. El Harti, A. Jellouli, and L. M. El Mostafa Bachaoui, "Lithological mapping using Landsat 8 anti atlas data in the bas drâa inlier, Moroccan OLI and Terra ASTER multispectral," *J. Appl. Remote Sens.*, vol. 10, no. 2, p. 15, 2016, doi: 10.1117/1.JRS.10.

[15] W. Ge, Q. Cheng, Y. Tang, L. Jing, and C. Gao, "Lithological classification using Sentinel-2A data in the Shibanjing ophiolite complex in Inner Mongolia, China," *Remote Sens.*, vol. 10, no. 4, p. 638, 2018, doi: 10.3390/rs10040638.

[16] V. Cortes and C. Vapnik, "Support-vector networks," *Mach. Learn.*, vol. 20, no. 3, pp. 273–297, 1992, doi: 10.1109/64.163674.

[17] T.-X. Zhang, J.-Y. Su, C.-J. Liu, and W.-H. Chen, "Potential bands of Sentinel-2A satellite for classification problems in precision agriculture," *Int. J. Autom. Comput.*, vol. 16, no. 1, pp. 16–26, Feb. 2019, doi: 10.1007/s11633-018-1143-x.

[18] S. Salati, F. J. A. van Ruitenbeek, F. D. van der Meer, M. H. Tangestani, and H. van der Werff, "Lithological mapping and fuzzy set theory: Automated extraction of lithological boundary from ASTER imagery by template matching and spatial accuracy assessment," *Int. J. Appl. Earth Observ. Geoinf.*, vol. 13, no. 5, pp. 753–765, Oct. 2011, doi: 10.1016/j.jag.2011.05.004.

[19] D. W. Leverington and W. M. Moon, "Landsat-TM-based discrimination of lithological units associated with the purtuniq ophiolite, Quebec, Canada," *Remote Sens.*, vol. 4, no. 5, pp. 1208–1231, May 2012, doi: 10.3390/rs4051208.

[20] T. L. Bowers and L. C. Rowan, "Remote mineralogic and lithologic mapping of the Ice River alkaline complex, British Columbia, Canada, using AVIRIS data," *Photogramm. Eng. Remote Sens.*, vol. 62, no. 12, pp. 1379–1385, 1996.

[21] R. Nijhawan, P. Garg, and P. Thakur, "A comparison of classification techniques for glacier change detection using multispectral images," *Perspect. Sci.*, vol. 8, pp. 377–380, Sep. 2016, doi: 10.1016/j.pisc.2016.04.080.

[22] S. Verbeiren, H. Eerens, I. Piccard, I. Bauwens, and J. Van Orshoven, "Sub-pixel classification of SPOT-VEGETATION time series for the assessment of regional crop areas in Belgium," *Int. J. Appl. Earth Observ. Geoinf.*, vol. 10, no. 4, pp. 486–497, Dec. 2008, doi: 10.1016/j.jag.2006.12.003.

[23] P. Dimitrov, Q. Dong, H. Eerens, A. Gikov, L. Filchev, E. Roumenina, and G. Jelev, "Sub-pixel crop type classification using PROBA-V 100 m NDVI time series and reference data from Sentinel-2 classifications," *Remote Sens.*, vol. 11, no. 11, p. 1370, Jun. 2019, doi: 10.3390/rs11111370.

[24] E. A. Addink, F. M. B. Van Coillie, and S. M. De Jong, "Introduction to the GEOBIA 2010 special issue: From pixels to geographic objects in remote sensing image analysis," *Int. J. Appl. Earth Observ. Geoinf.*, vol. 15, pp. 1–6, Apr. 2012, doi: 10.1016/j.jag.2011.12.001.

[25] P. Fisher, "The pixel: A snare and a delusion," *Int. J. Remote Sens.*, vol. 18, no. 3, pp. 679–685, 1997, doi: 10.1080/014311697219015.

[26] L. Drăguţ and T. Blaschke, "Automated classification of landform elements using object-based image analysis," *Geomorphology*, vol. 81, nos. 3–4, pp. 330–344, Nov. 2006, doi: 10.1016/j.geomorph.2006.04.013.

[27] M. D. Hossain and D. Chen, "Segmentation for object-based image analysis (OBIA): A review of algorithms and challenges from remote sensing perspective," *ISPRS J. Photogram. Remote Sens.*, vol. 150, pp. 115–134, Apr. 2019, doi: 10.1016/j.isprsjprs.2019.02.009.

[28] M. Baatz, "Baatz, Schäpe_2000_multiresolution segmentation an optimization approach for high quality multi-scale image segmentation.pdf," in *Angewandte Geographische Informationsverarbeitung XII*, vol. 58. 2000, pp. 12–23.

[29] T. Blaschke, "Object based image analysis for remote sensing," *ISPRS J. Photogram. Remote Sens.*, vol. 65, no. 1, pp. 2–16, Jan. 2010, doi: 10.1016/j.isprsjprs.2009.06.004.

[30] S. Imane, R. Mohamed, and H. Mustapha, "A comparison of GEOBIA vs PBIA machine learning methods for lithological mapping using Sentinel 2 imagery: Case study of Skhour Rehamna, Morocco," in *Proc. IEEE Int. Conf. Moroccan Geomatics (Morgeo)*, May 2020, pp. 2–7, doi: 10.1109/Morgeo49228.2020.9121899.

[31] Y. Qian, W. Zhou, J. Yan, W. Li, and L. Han, "Comparing machine learning classifiers for object-based land cover classification using very high resolution imagery," *Remote Sens.*, vol. 7, no. 1, pp. 153–168, Dec. 2014, doi: 10.3390/rs70100153.

[32] L. Ma, M. Li, X. Ma, L. Cheng, P. Du, and Y. Liu, "A review of supervised object-based land-cover image classification," *ISPRS J. Photogramm. Remote Sens.*, vol. 130, pp. 277–293, Aug. 2017, doi: 10.1016/j.isprsjprs.2017.06.001.

[33] E. A. Waspadi and P. Danoedoro, "Comparing per-pixel and object-based classification results using two different land-cover/land-use classification schemes: A case study using Landsat-8 OLI imagery," *Proc. SPIE*, vol. 1137206, Dec. 2019, Art. no. 1137206, doi: 10.1117/12.2541876.

[34] D. Hölbling, B. Friedl, and C. Eisank, "An object-based approach for semi-automated landslide change detection and attribution of changes to landslide classes in Northern Taiwan," *Earth Sci. Informat.*, vol. 8, no. 2, pp. 327–335, Jun. 2015, doi: 10.1007/s12145-015-0217-3.

[35] P. Lightfoot, C. Scott, and C. Fitzsimmons, "Using object-based image analysis with multi-temporal aerial imagery and LiDAR to detect change in temperate intertidal habitats," *Aquatic Conservation, Mar. Freshwater Ecosyst.*, vol. 30, no. 3, pp. 514–531, Mar. 2020, doi: 10.1002/aqc.3277.

[36] R. Momeni, P. Aplin, and D. Boyd, "Mapping complex urban land cover from spaceborne imagery: The influence of spatial resolution, spectral band set and classification approach," *Remote Sens.*, vol. 8, no. 2, p. 88, Jan. 2016, doi: 10.3390/rs8020088.

[37] A. A. Case, "Classification of landforms for digital soil mapping in urban areas using LiDAR data derived terrain attributes: A case study from Berlin, Germany," *Land*, vol. 9, no. 9, p. 319, 2020.

[38] A. Lucieer and A. Stein, "Texture-based landform segmentation of LiDAR imagery," *Int. J. Appl. Earth Observ. Geoinf.*, vol. 6, nos. 3–4, pp. 261–270, Mar. 2005, doi: 10.1016/j.jag.2004.10.008.

[39] L. Drăguţ and C. Eisank, "Automated object-based classification of topography from SRTM data," *Geomorphology*, vols. 141–142, pp. 21–33, Mar. 2012, doi: 10.1016/j.geomorph.2011.12.001.

[40] S. Grebby, E. Field, and K. Tansey, "Evaluating the use of an object-based approach to lithological mapping in vegetated terrain," *Remote Sens.*, vol. 8, no. 10, p. 843, 2016, doi: 10.3390/rs8100843.

[41] S. Shayeganpour, M. H. Tangestani, S. Homayouni, and R. K. Vincent, "Evaluating pixel-based vs. object-based image analysis approaches for lithological discrimination using VNIR data of WorldView-3," *Frontiers Earth Sci.*, vol. 15, no. 1, pp. 38–53, Mar. 2021, doi: 10.1007/s11707-020-0848-7.

[42] M. H. Tangestani and S. Shayeganpour, "Mapping a lithologically complex terrain using Sentinel-2A data: A case study of Suriyan area, southwestern Iran," *Int. J. Remote Sens.*, vol. 41, no. 9, pp. 3558–3574, May 2020, doi: 10.1080/01431161.2019.1706203.

[43] C. Kumar, A. Shetty, S. Raval, R. Sharma, and P. K. C. Ray, "Lithological discrimination and mapping using ASTER SWIR data in the Udaipur area of Rajasthan, India," *Procedia Earth Planet. Sci.*, vol. 11, pp. 180–188, Jan. 2015, doi: 10.1016/j.proeps.2015.06.022.

[44] F. Al-Nahmi, O. Saddiqi, A. Hilali, H. Rhinane, L. Baidder, H. El Arabi, and K. Khanbari, "Application of remote sensing in geological mapping, case study al maghrabah area–Hajjah Region, Yemen," *ISPRS Ann. Photogramm., Remote Sens. Spatial Inf. Sci.*, vol. IV–4/W4, pp. 63–71, Nov. 2017, doi: 10.5194/isprs-annals-IV-4-W4-63-2017.

[45] W. Ge, Q. Cheng, L. Jing, F. Wang, M. Zhao, and H. Ding, "Assessment of the capability of Sentinel-2 imagery for iron-bearing minerals mapping: A case study in the cuprite area, Nevada," *Remote Sens.*, vol. 12, no. 18, p. 3028, Sep. 2020, doi: 10.3390/RS12183028.

[46] M. W. Mwaniki, M. S. Matthias, and G. Schellmann, "Application of remote sensing technologies to map the structural geology of central region of Kenya," *IEEE J. Sel. Topics Appl. Earth Observ. Remote Sens.*, vol. 8, no. 4, pp. 1855–1867, Apr. 2015, doi: 10.1109/JSTARS.2015.2395094.

[47] C. Kumar, S. Chatterjee, T. Oommen, and A. Guha, "Automated lithological mapping by integrating spectral enhancement techniques and machine learning algorithms using AVIRIS-NG hyperspectral data in gold-bearing granite-greenstone rocks in Hutti, India," *Int. J. Appl. Earth Observ. Geoinf.*, vol. 86, Apr. 2020, Art. no. 102006, doi: 10.1016/j.jag.2019.102006.

[48] G. I. Metternicht and A. Fermont, "Estimating erosion surface features by linear mixture modeling," *Remote Sens. Environ.*, vol. 64, no. 3, pp. 254–265, 1998, doi: 10.1016/S0034-4257(97)00172-7.

[49] R. G. Bryant, "Validated linear mixture modelling of Landsat TM data for mapping evaporite minerals on a Playa surface: Methods and applications," *Int. J. Remote Sens.*, vol. 17, no. 2, pp. 315–330, Jan. 1996, doi: 10.1080/01431169608949008.

[50] T. Baudin, P. Chèvremont, P. Razin, N. Youbi, D. Andries, D. Thiéblemont, E. M. Chihani, and M. Tegyey, "Carte géologique du Maroc au 1/50 000, feuille de Skhour des Rehamna, Mémoire explicatif," in *Notes et Mémoires du Service Géologique du Maroc N 435 Bis*. 2003.

[51] F. Chopin, M. Corsini, K. Schulmann, M. El Houicha, J. F. Ghienne, and J. B. Edel, "Tectonic evolution of the Rehamna metamorphic dome (Morocco) in the context of the Alleghanian-Variscan orogeny," *Agupublications*, vol. 33, no. 6, pp. 1154–1177, 2014.

[52] A. M. Aghzer and R. Arenas, "Evolution metamorphique des metapelites du Massif hercynien des Rehamna (Maroc): Implications tectonothermales," *J. Afr. Earth Sci.*, vol. 27, no. 1, pp. 87–106, 1998, doi: 10.1016/S0899-5362(98)00048-7.

[53] A. A. Mouhsine, "Evolution tectonothermale du massif hercynien des Rehamna (zone centre-mesetienne, maroc)," Tectonique. Universidad Complutense de Madrid, French, 1994.

[54] P. Jenny, *Contribution à la Géologie Structurale des Rehamna (Meseta Marocaine Méridionale). Le Matériel Paléozoéque et Son évolution Hercynienne Dans le Centre Du Massif*. Strasbourg, France: Univ. Louis Pasteur, 1974, p. 120.

[55] C. Hoepffner, "Contribution à la géologie structurale des Rehamna (meseta marocaine méridionale), le matériel paléozoïque et son évolution hercynienne dans l'est du massif. Tectonique," Université Louis Pasteur—Strasbourg I, French, 1974.

[56] J. Louis, V. Debaecker, B. Pflug, M. Main-Knorn, J. Bieniarz, U. Mueller-Wilm, E. Cadau, and F. Gascon, "Sentinel-2 SEN2COR: L2A processor for users," in *Proc. Living Planet Symp.*, vol. SP-740, Aug. 2016, pp. 9–13.

[57] C. Bouzinac, O. Thépaut, M. Jung, B. Francesconi, J. Louis, V. Lonjou, B. Lafrance, S. Massera, A. Gaudel-Vacaresse, and F. Languille, "Copernicus Sentinel-2A calibration and products validation status," *Remote Sens.*, vol. 9, no. 6, p. 584, Jun. 2017, doi: 10.3390/rs9060584.

[58] *Sentinel-2 User Handbook, Issue 1 Revision 2*, European Space Agency, Paris, France, 1956, vol. 48, no. 9.

[59] E. M. B. Z. Adiri, A. E. Harti, A. Jellouli, and L. Maacha, "Lithological mapping using Landsat 8 OLI and Terra ASTER multispectral data in the Bas Drâa inlier, Moroccan Anti Atlas," *J. Appl. Remote Sens.*, vol. 10, no. 2, 2016, Art. no. 036012, doi: 10.1117/1.JRS.10.

[60] M. M. Shokry, M. F. Sadek, A. F. Osman, and B. A. El Kalioubi, "Precambrian basement rocks of Wadi-Khuda-Shut area, South Eastern Desert of Egypt: Geology and remote sensing analysis," *Egyptian J. Remote Sens. Space Sci.*, vol. 24, no. 1, pp. 59–75, Feb. 2021, doi: 10.1016/j.ejrs.2019.12.005.

[61] S. A. Drury and S. M. Berhe, "Accretion tectonics in northern Eritrea revealed by remotely sensed imagery," *Geolog. Mag.*, vol. 130, no. 2, pp. 177–190, Mar. 1993, doi: 10.1017/S0016756800009845.

[62] S. D. Khan, K. Mahmood, and J. F. Casey, "Mapping of muslim Bagh Ophiolite complex (Pakistan) using new remote sensing, and field data," *J. Asian Earth Sci.*, vol. 30, no. 2, pp. 333–343, Apr. 2007, doi: 10.1016/j.jseaes.2006.11.001.

[63] M. Pournamdari, M. Hashim, and A. B. Pour, "Spectral transformation of ASTER and Landsat TM bands for lithological mapping of Soghan Ophiolite complex, South Iran," *Adv. Space Res.*, vol. 54, no. 4, pp. 694–709, Aug. 2014, doi: 10.1016/j.asr.2014.04.022.

[64] A. Hyvärinen, "Independent component analysis: Recent advances," *Phil. Trans. Roy. Soc. A, Math., Phys. Eng. Sci.*, vol. 371, no. 1984, Feb. 2013, Art. no. 20110534, doi: 10.1098/rsta.2011.0534.

[65] C. S. Bravo and A. H. de Egaña Espinosa de los Monteros, "The influences of the downsizing strategy on business structures," *Rev. Bus. Manage.*, vol. 19, no. 63, pp. 118–132, Feb. 2017, doi: 10.7819/rbgn.v19i63.1905.

[66] H. P. A. Hyvärinen, K. Zhang, and S. Shimizu, "Estimation of a structural vector autoregression model using non-Gaussianity," *J. Mach. Learn. Res.*, vol. 10, no. 1, pp. 1709–1731, 2010, doi: 10.1016/j.eneco.2014.12.001.

[67] S. Shimizu, "Joint estimation of linear non-Gaussian acyclic models," *Neurocomputing*, vol. 81, pp. 104–107, Apr. 2012, doi: 10.1016/j.neucom.2011.11.005.

[68] C. H. Chen and X. Zhang, "Independent component analysis for remote sensing study," *Proc. SPIE*, vol. 3871, pp. 150–158, Sep. 1999.

[69] B. Bahrambeygi and H. Moeinzadeh, "Comparison of support vector machine and neutral network classification method in hyperspectral mapping of ophiolite mélanges—A case study of East of Iran," *Egyptian J. Remote Sens. Space Sci.*, vol. 20, no. 1, pp. 1–10, Jun. 2017, doi: 10.1016/j.ejrs.2017.01.007.

[70] A. Othman and R. Gloaguen, "Improving lithological mapping by SVM classification of spectral and morphological features: The discovery of a new chromite body in the Mawat Ophiolite complex (Kurdistan, NE Iraq)," *Remote Sens.*, vol. 6, no. 8, pp. 6867–6896, Jul. 2014, doi: 10.3390/rs6086867.

[71] A. Gasmi, C. Gomez, H. Zouari, A. Masse, and D. Ducrot, "PCA and SVM as geo-computational methods for geological mapping in the southern of Tunisia, using ASTER remote sensing data set," *Arabian J. Geosci.*, vol. 9, no. 20, pp. 1–12, Dec. 2016, doi: 10.1007/s12517-016-2791-1.

[72] A. Vapnik, and V. Chervonenkis, "The necessary and sufficient conditions for consistency in the empirical risk minimization method," *Image Anal*, vol. 1, no. 3, pp. 283–305, 1991.

[73] N. I. S. Bahari, A. Ahmad, and B. M. Aboobaider, "Application of support vector machine for classification of multispectral data," *IOP Conf. Ser. Earth Environ. Sci.*, vol. 20, no. 1, 2014, Art. no. 012038, doi: 10.1088/1755-1315/20/1/012038.

[74] A. Tzotsos and D. Argialas, "MSEG: A generic region-based multi-scale image segmentation algorithm for remote sensing imagery," in *Proc. ASPRS Annu. Conf.*, vol. 3, May 2006, pp. 1485–1497.

[75] P. Mantero, G. Moser, and S. B. Serpico, "Partially supervised classification of remote sensing images using SVM-based probability density estimation," in *Proc. IEEE Workshop Adv. Techn. Anal. Remotely Sensed Data*, Oct. 2004, pp. 327–336, doi: 10.1109/WARSD.2003.1295212.

[76] B. Fowler, "A sociological analysis of the satanic verses affair," *Theory, Culture Soc.*, vol. 17, no. 1, pp. 39–61, Feb. 2000, doi: 10.1177/02632760022050997.

[77] C. Huang, L. S. Davis, and J. R. G. Townshend, "An assessment of support vector machines for land cover classification," *Int. J. Remote Sens.*, vol. 23, no. 4, pp. 725–749, 2002.

[78] P. T. Noi and M. Kappas, "Comparison of random forest, k-nearest neighbor, and support vector machine classifiers for land cover classification using Sentinel-2 imagery," *Sensors*, vol. 18, no. 2, p. 18, Dec. 2017, doi: 10.3390/s18010018.

[79] P. Casals-Carrasco, S. Kubo, and B. B. Madhavan, "Application of spectral mixture analysis for terrain evaluation studies," *Int. J. Remote Sens.*, vol. 21, no. 16, pp. 3039–3055, Jan. 2000, doi: 10.1080/01431160050144947.

[80] Y. Chen and W. Wu, "Mapping mineral prospectivity using an extreme learning machine regression," *Ore Geol. Rev.*, vol. 80, pp. 200–213, Jan. 2017, doi: 10.1016/j.oregeorev.2016.06.033.

[81] I. Bachri, M. Hakdaoui, M. Raji, A. C. Teodoro, and A. Benbouziane, "Machine learning algorithms for automatic lithological mapping using remote sensing data: A case study from Souk Arbaa Sahel, Sidi Ifni Inlier, Western Anti-Atlas, Morocco," *ISPRS Int. J. Geo-Inf.*, vol. 8, no. 6, pp. 1–20, 2019, doi: 10.3390/ijgi8060248.

[82] S. Esmaeili, M. H. Tangestani, and M. H. Tayebi, "Sub-pixel mapping of Copper- and iron-bearing metamorphic rocks using ASTER data: A case study of Toutak and Surian complexes, NE Shiraz, Iran," *Natural Resour. Res.*, vol. 29, no. 5, pp. 2933–2948, Oct. 2020, doi: 10.1007/s11053-020-09639-x.

[83] C. Kumar, A. Shetty, S. Raval, P. K. Champatiray, and R. Sharma, "Sub-pixel mineral mapping using EO-1 hyperion hyperspectral data," *Int. Arch. Photogramm. Remote Sens. Spat. Inf. Sci. ISPRS Arch.*, vol. XL-8, no. 1, pp. 455–461, 2014, doi: 10.5194/isprsarchives-XL-8-455-2014.

[84] M. Hosseinjani and M. H. Tangestani, "Mapping alteration minerals using sub-pixel unmixing of ASTER data in the Sarduiyeh area, SE Kerman, Iran," *Int. J. Digit. Earth*, vol. 4, no. 6, pp. 487–504, Nov. 2011, doi: 10.1080/17538947.2010.550937.

[85] K. C. Mertens, B. De Baets, L. P. C. Verbeke, and R. R. De Wulf, "Direct sub-pixel mapping exploiting spatial dependence," in *Proc. IEEE Int. Geosci. Remote Sens. Symp., (IGARSS)*, Sep. 2004, pp. 3046–3049, doi: 10.1109/igarss.2004.1370340.

[86] R. C. Weih and N. D. Riggan, "Object-based classification vs. pixel-based classification: Comparitive importance of multi-resolution imagery," *Int. Arch. Photogramm. Remote Sens. Spat. Inf. Sci.*, vol. 38, no. 4, pp. 1–6, 2010.

[87] M. Flanagan and D. L. Civco, "Imagine subpixel classifier version 8.4," *Photogramm. Eng. Remote S*, vol. 67, pp. 23–28, 2001.

[88] J. R. Harris, R. McGregor, and P. Budkewitsch, "Geological analysis of hyperspectral data over southwest Baffin island: Methods for producing spectral maps that relate to variations in surface lithologies," *Can. J. Remote Sens.*, vol. 36, no. 4, pp. 412–435, Jan. 2010, doi: 10.5589/m10-072.

[89] T. Blaschke, G. J. Hay, M. Kelly, S. Lang, P. Hofmann, E. Addink, R. Q. Feitosa, F. van der Meer, H. van der Werff, F. van Coillie, and D. Tiede, "Geographic object-based image analysis—Towards a new paradigm," *ISPRS J. Photogramm. Remote Sens.*, vol. 87, pp. 180–191, Jan. 2014, doi: 10.1016/j.isprsjprs.2013.09.014.

[90] U. C. Benz, P. Hofmann, G. Willhauck, I. Lingenfelder, and M. Heynen, "Multi-resolution, object-oriented fuzzy analysis of remote sensing data for GIS-ready information," *ISPRS J. Photogramm. Remote Sens.*, vol. 58, nos. 3–4, pp. 239–258, Jan. 2004, doi: 10.1016/j.isprsjprs.2003.10.002.

[91] M. Baatz and A. Schäpe, "Multiresolution segmentation: An optimization approach for high quality multi-scale image segmentation," in *Angewandte Geographische Informationsverarbeitung XII*, vol. 58. 2000, pp. 12–23.

[92] G. Willhauck and T. Schneider, "Oriented classification techniques and standard image analysis for the use of change detection between SPOT multispectral satellite images and aerial photos," in *Proc. XIX ISPRS*, vol. 33, 2000, pp. 214–221. [Online]. Available: http://citeseerx.ist.psu.edu/viewdoc/download?doi=10.1.1.203.1868&rep=rep1&type=pdf

[93] D. C. Duro, S. E. Franklin, and M. G. Dubé, "A comparison of pixel-based and object-based image analysis with selected machine learning algorithms for the classification of agricultural landscapes using SPOT-5 HRG imagery," *Remote Sens. Environ.*, vol. 118, pp. 259–272, Mar. 2012, doi: 10.1016/j.rse.2011.11.020.

[94] R. G. Congalton, "A review of assessing the accuracy of classifications of remotely sensed data," *Remote Sens. Environ.*, vol. 37, no. 1, pp. 35–46, 1991, doi: 10.1016/0034-4257(91)90048-B.

[95] S. Lang, "Object-based image analysis for remote sensing applications: Modeling reality—Dealing with complexity," in *Object-Based Image Analysis* (Lecture Notes in Geoinformation and Cartography), T. Blaschke, S. Lang, and G. J. Hay, Eds. Berlin, Germany: Springer, 2008, doi: 10.1007/978-3-540-77058-9_1.

[96] M. S. Tehrany, B. Pradhan, and M. N. Jebuv, "A comparative assessment between object and pixel-based classification approaches for land use/land cover mapping using SPOT 5 imagery," *Geocarto Int.*, vol. 29, no. 4, pp. 351–369, May 2014, doi: 10.1080/10106049.2013.768300.
[97] B. Pradhan and Z. Suleiman, "Landcover mapping and spectral analysis using multi-sensor satellite data fusion techniques: Case study in Tioman Island, Malaysia," *J. Geomatics*, vol. 3, no. 2, pp. 71–78, 2009.
[98] A. R. Gullickson, "Accuracy standards," in *The Student Evaluation Standards*. Newbury Park, CA, USA: Sage, 2003, pp. 125–208, doi: 10.4135/9781412990097.

IMANE SERBOUTI was born in Settat, Casablanca-Settat, Morocco, in 1994. She received the B.Sc. degree in mineral resources and quarries from the Faculty of Sciences and Techniques, University Hassan I, Settat, in 2015, and the M.Sc. degree in GIS and remote sensing applied to geosciences and environment from the Faculty of Sciences Ben M'sik, University Hassan II, Casablanca, in 2017, where she is currently pursuing the Ph.D. degree with the Laboratory of Applied Geology, Geomatics and Environment. Her research interests include the application of advanced machine learning approaches cloud computing and deep learning for remote sensing image classification, and geological mapping.

MOHAMMED RAJI was born in Casablanca, Morocco, in 1959. He received the 3rd cycle Ph.D. degree in structural geology from Caddi Ayad University, Marrakech, Morocco, in 1988, and the State Ph.D. degree in structural geology from Hassan II University of Casablanca, Morocco, in 2007. From 2007 to 2021, he was worked as a Professor Researcher with the Hassan II University of Casablanca. He was the Geology Head of the Department, from 2008 to 2010, and from 2018 to 2020. He was also the Adjoint-Director of the Laboratory of Applied Geology, Geomatics and Environment, Faculty of Sciences Ben M'Sik, Hassan II University, Casablanca, from 2014 to 2017. Since 2007, he has been a Professor Master Assistant. His research interests include the application of remote sensing, particularly machine and deep learning methods, and in structural and geological mapping.

MUSTAPHA HAKDAOUI was born in Casablanca, Morocco, in 1958. He received the DEA and DESS degrees in geophysics and remote sensing from the University of Paris VI and Paris VII, in 1984 and 1986, respectively, and the Ph.D. degree in processing and textural analysis of spatial images from Pierre and Marie Curie University, in 1991. From 1991 to 2021, he was a Professor with the Laboratory of Applied Geology, Geomatics and Environment, Faculty of sciences Ben M'sik, Hassan II University, Casablanca. He is the author of more than 50 articles and more than 70 communications. His research interests include artificial intelligence approaches, image classifications by machine learning, and deep learning algorithms for thematic and more particularly geological mapping.

BISWAJEET PRADHAN (Senior Member, IEEE) received the Habilitation degree in remote sensing from the Dresden University of Technology, Germany, in 2011. He is currently the Director of the Centre for Advanced Modelling and Geospatial Information Systems (CAMGIS), Faculty of Engineering and IT. He is also a Distinguished Professor with the University of Technology Sydney. He is also an Internationally Established Scientist in the fields of geospatial information systems (GIS), remote sensing and image processing, complex modeling/geo-computing, machine learning and soft-computing applications, natural hazards, and environmental modeling. Out of his more than 650 articles, more than 500 have been published in science citation index (SCI/SCIE) technical journals. He has authored eight books and 13 book chapters. From 2015 to 2021, he served as the Ambassador Scientist for the Alexander Humboldt Foundation, Germany. He was a recipient of the Alexander von Humboldt Fellowship from Germany. He has received 55 awards in recognition of his excellence in teaching, service, and research, from 2006. He was also a recipient of the Alexander von Humboldt Research Fellowship from Germany. From 2016 to 2020, he was listed as the World's Most Highly Cited Researcher by Clarivate Analytics Report as one of the world's most influential mind. From 2018 to 2020, he was awarded as the World Class Professor by the Ministry of Research, Technology and Higher Education, and Indonesia. He is also an Associate Editor and an Editorial Member of more than eight ISI journals. He has widely traveled abroad, visiting more than 52 countries to present his research findings.

CHANG-WOOK LEE (Member, IEEE) received the B.S. degree from Kangwon National University, Chuncheon, South Korea, and the M.S. and Ph.D. degrees from Yonsei University, Seoul, South Korea, in 1999 and 2009, respectively. He held a postdoctoral position in InSAR for the ARTS contract with the U.S. Geological Survey EROS data center, and all work was to be performed as determined by the USGS Project Manager working in coordination with SSSC Management. The work was performed at the USGS Cascades Volcano Observatory in Vancouver, Washington, by the National Aeronautics and Space Administration (NASA) project supports from 2009 to 2011. He is currently an Associate Professor with the Department of Science of Education, Kangwon National University. He has authored more than 100 articles in these research fields. His research interests include SAR, InSAR, and time-series processing technique development on natural disaster monitoring and resource characterization.

ABDULLAH M. ALAMRI received the B.S. degree in geology from King Saud University, in 1981, the M.Sc. degree in applied geophysics from the University of South Florida, Tampa, in 1985, the M.S. degree from King Saud University, and the Ph.D. degree in earthquake seismology from University of Minnesota, USA, in 1990. He is currently a Professor of earthquake seismology, the Director of the Seismic Studies Center, King Saud University (KSU). He is also the President of the Saudi Society of Geosciences and the Editor-in-Chief of the Arabian Journal of Geosciences (AJGS). He has published more than 150 research papers, achieved more than 45 research projects as well as authored several books and technical reports. His research interests are in the area of crustal structures and seismic micro zoning of the Arabian Peninsula. His recent projects involve also applications of EM and MT in deep groundwater exploration of Empty Quarter and geothermal prospecting of volcanic Harrats in the Arabian shield. He is a member of Seismological Society of America, American Geophysical Union, European Assistant for Environmental and Engineering Geophysics, Earthquakes Mitigation in the Eastern Mediterranean Region, National Comm. for Assessment & Mitigation of Earthquake Hazards in Saudi Arabia, Mitigation of Natural Hazards Com at Civil Defense. He is the Principal and the Co-Investigator in several national and international projects (KSU, KACST, NPST, IRIS, CTBTO, US Air force, NSF, UCSD, LLNL, OSU, PSU, and Max Planck). He has also chaired and co-chaired several SSG, GSF, and RELEMR workshops and forums in the Middle East. He obtained several worldwide prizes and awards for his scientific excellence and innovation.